A Comprehensive Kinetic Study of Thermal Reduction of NO$_2$ by H$_2$

J. Park, Nevia D. Giles,[†] Jesse Moore,[†] and M. C. Lin*

Department of Chemistry, Emory University, Atlanta, Georgia 30322

Received: July 23, 1998; In Final Form: October 5, 1998

A comprehensive study of the kinetics and mechanism for the thermal reduction of NO$_2$ by H$_2$ has been carried out in the temperature range 602−954 K by pyrolysis/FTIR spectrometry employing different mixtures containing (1) NO$_2$/Ar, (2) NO$_2$/NO/Ar, (3) NO$_2$/H$_2$/Ar, (4) NO$_2$/H$_2$/CO/Ar, and (5) NO$_2$/H$_2$/CO/NO/Ar. The results of kinetic modeling for the data obtained from mixtures 1 and 2 gave the rate constant for the key reaction responsible for NO formation and NO$_2$ decay, 2NO$_2$ → 2NO + O$_2$ (4): $k_4 = 4.16 \times 10^{12}$ exp($-13\ 840/T$) cm^3/(mol s). Combination of our data with those of Röhrig et al. (ref 27) measured at high temperatures in shock waves led to $k_4 = (4.51 \pm 0.15) \times 10^{12}$ exp[$-(13\ 890 \pm 27)/T$] cm^3/(mol s) for 600 K < T < 1450 K. Kinetic modeling of the measured data from mixtures 3−5 indicated that the existing rate constant for H$_2$ + NO$_2$ → HONO + H (−1) was too large; on the other hand, our theoretically predicted rate constant, $k_{-1} = (1.30 \times 10^4)T^{2.76}$ exp($-14\ 980/T$) cm^3/(mol s), obtained by high-level ab initio MO/TST calculations with a small adjustment for the computed barrier from 32.5 to 33.0 kcal/mol, can quantitatively account for measured concentrations of NO$_x$ and CO$_x$ (in CO-added experiment), $x = 1$ and 2, and for NO$_2$ decay rates reported earlier by Ashmore and Levitt (ref 22).

1. Introduction

In a recent series of experimental[1−8] and theoretical[9−21] studies, we have attempted to elucidate the complex chemistry of systems containing H/N/O species, including NH$_x$, NO$_x$, and HNO$_x$ ($x = 1-3$). These species are relevant to the formation and reduction of nitrogen oxide pollutants as well as to the combustion of high-energy nitramine molecules.

As HONO (nitrous acid) plays a pivotal role in these H/N/O systems both as the OH radical source (by fragmentation) and as a radical scavenger (by the X + HONO → HX + NO$_2$ reactions), we have investigated its reactions with H, OH, NO, and NH$_2$ by ab initio MO/statistical theory calculations.[20] In addition, the rate constants for the oxidation of HNO by NO$_2$ producing HONO and the bimolecular self-reaction, HONO + HONO → NO + NO$_2$ + H$_2$O, both of which were not experimentally measured reliably, have been computed theoretically.[18,19]

To test our state of understanding the H/N/O chemistry vis-à-vis the HONO kinetics, we have recently carried out a computer modeling of the kinetic data obtained some time ago by Ashmore and Levitt[22] on the thermal reduction of NO$_2$ by H$_2$ with and without added NO as a radical scavenger. The dashed curves in Figure 1 show the results of our modeling using recommended rate constants[23] for the key reactions involving HONO with the mechanism summarized in the Appendix. As revealed by the results presented in the figure, the existing kinetics for HONO reactions cannot account for the measured NO$_2$ decay rates under the conditions studied; neither can our newly measured kinetic data be reasonably explained by means of the existing key rate constants for these reactions (vide infra). The failure in our ability to simulate the kinetics of this relatively simple system suggests the need for the aforementioned theoretical studies on the HONO reactions
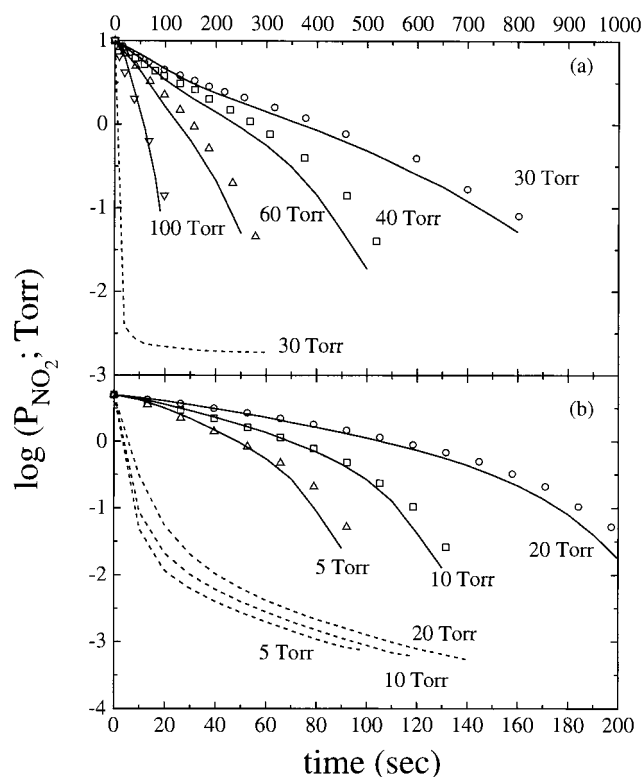

Figure 1. (a) The decay of P_{NO2} with time, all runs have 10 Torr of NO$_2$ and the indicated pressures of H$_2$; temperature at 684 K. (b) The inhibition effect of NO: 5 Torr of NO$_2$ and 100 Torr of H$_2$, with the indicated pressures of NO. (—) Modeled results using our k_{-1} and k_7 values; (- - -), modeled results using the recommended rate constants for k_{-1} and k_7 (sec the Appendix). Data were reproduced from ref 22.

and for additional, more reliable, kinetic measurements for characterization of some of these reactions.

In the H$_2$−NO$_2$ system, the multichannel elementary processes involving the reaction of H and HONO via various

---

* Corresponding author. E-mail: chemmcl@emory.edu.
† High-school summer apprentice.

TABLE 1: Experimental Conditions^a in P/FTIR Experiment for the Reaction of H_2 + NO_2

	temp (K)	time (s)	$[H_2]_o$	$[NO_2]_o$	$[NO]_o$	$[CO]_o$
Figure 3a	703−954	900		3.17		
Figure 3b	625−910	1200		4.02	2.06	
Figure 6a	602−690	1200	11.8	1.75		
Figure 6b	646−774	1200	3.74	3.80		
Figure 7a	652−746	1200	8.23	4.01	3.41	3.28
Figure 7b	623−709	1200	5.38	5.37		4.47

^{a} The partial pressures for each reactant are given in Torr, and all experiments were carried out at 760 Torr total pressure.

product channels

$$H + HONO \rightleftarrows H_2 + NO_2 \qquad (1, -1)$$

$$\rightleftarrows OH + HNO \qquad (2, -2)$$

$$\rightleftarrows H_2O + NO \qquad (3, -3)$$

play a particularly important role in the chain-initiation (reaction −1), chain-branching (reaction 2), and chain termination (reaction 3). The rate constants for all reaction channels have been computed by means of high-level ab initio MO/statistical theory caculations.[17]

In the present study, we pyrolyze mixtures of H_2 and NO_2 with and without added CO. As CO is a known OH scavenger through the well-established reaction OH + CO → CO_2 + H, the absolute concentration of the CO_2 formed in the reaction allows us to monitor the amount of the OH radical, the key chain carrier in the present system. By measuring the absolute concentrations of NO, NO_2, CO, and CO_2 by FTIR spectrometry as functions of temperature and the partial pressures of the reactants, we should be able to identify the key processes involving HONO (as alluded to above) which control the reduction of NO_2 by H_2.

2. Experimental Section

The thermal reaction of NO_2 with and without reactive additives (H_2, NO, and CO) was carried out in a 270-mL quartz reactor, which was resistively heated with a double-walled cylindrical furnace. The furnace was heated and controlled by a solid-state temperature controller. Reaction temperature was measured to ±0.5 K with a thermocouple placed in a capillary tube vacuum sealed at the center of the reactor. The detailed experimental procedure of the pyrolysis/FTIR spectrometric technique can be found in our earlier studies.[24−26]

Pyrolyzed or unpyrolyzed reference samples were expanded into the absorption cell inside the analysis chamber of the FTIR spectrometer (Mattson Instruments, Polaris) for determination of the concentrations of the products and the unreacted reactants with a resolution of 4 cm^{-1}. The absolute concentrations of the reactants and products of pyrolyzed and unpyrolyzed samples were determined by standard calibration curves. The calibration curves were obtained with standard mixtures containing reactants and/or products at pressures near those of expanded, pyrolyzed samples by plotting in terms of concentration versus absorbance at 1627.8 cm^{-1} for NO_2, 1896.9 cm^{-1} for NO, 2172.7 cm^{-1} for CO, and 2358.8 cm^{-1} for CO_2. The pressures of the samples after expansion are approximately 280 Torr. To minimize the effect of pressure broadening, the pressure of calibration mixtures containing varying amounts of reactants and products was maintained at 280 ± 10 Torr.

Six different NO_2 mixtures with varying amounts of H_2, NO, and CO were employed in the study using Ar as the diluent. The compositions of these mixtures are given in Table 1. To
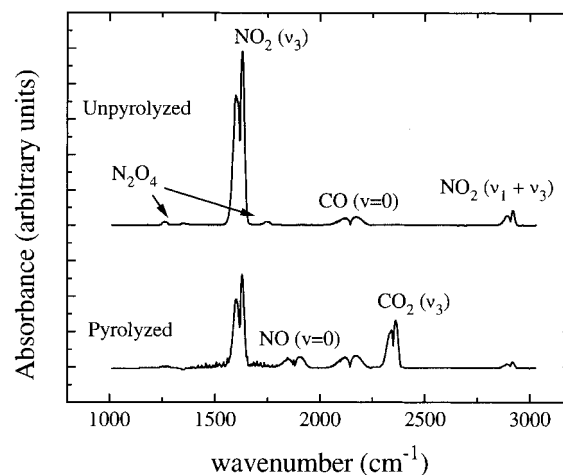

Figure 2. Typical FTIR spectra of pyrolyzed and unpyrolyzed mixtures of $H_2/NO_2/CO$. The pyrolyzed spectrum was expanded for better visibility.

ascertain that the bimolecular self-reactions of NO_2 can be quantitatively characterized in the absence of H_2 and CO, two mixtures containing NO_2/Ar and $NO_2/NO/Ar$ were pyrolyzed in the 703−954 and 625−910 K temperature ranges, respectively.

For the thermal reaction of NO_2 with H_2, four mixtures, two of them with added CO, were employed. The purpose for the addition of CO, as alluded to in the Introduction, is to monitor OH and convert it to H by the OH + CO reaction. Figure 2 shows a typical set of FTIR spectra obtained before and after the pyrolysis of a mixture containing NO_2, H_2, and CO. All experiments were performed at atmospheric pressure with a 1200 s resident time except those specified individually.

NO_2 (Aldrich) and CO_2 (Aldrich) were purified by standard trap-to-trap distillation. CO (Matheson) was purified by passing through two liquid N_2 traps (to remove CO_2 and H_2O), and NO (Matheson) was purified by vacuum distillation through a silica-gel trap maintained at 195 K to remove impurities such as NO_2. H_2 and Ar (99.9995%) were used without further purification.

3. Results

The reactant and product species concentrations after pyrolysis, at different reaction times and reactant compositions, under atmospheric-pressure conditions were measured as a function of temperature. The reaction temperature was from 600 to 954 K, and the compositions varied for the three types of reaction mixtures containing (1) NO_2 with or without NO, (2) NO_2 and H_2, and (3) NO_2, H_2, and CO, with or without NO, all using Ar as the diluent as specified in Table 1.

The NO_2/Ar mixtures were used to check the reliability of the rate constants for the reactions

$$NO_2 + NO_2 \rightleftarrows 2NO + O_2 \qquad (4)$$

$$NO_2 + NO_2 \rightleftarrows NO + NO_3 \qquad (5)$$
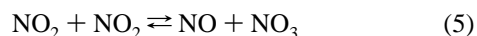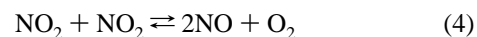
which dominate the production of NO, particularly reaction 4. Reaction 5 is less important than react 4 under our pyrolytic conditions because of the very fast reverse process (−5), which is also well-established.[23]

For this reaction system, the experimentally measured concentrations of NO and NO_2 at a specified reaction time are shown in Figure 3; they can be quantitatively modeled with the recommended rate constants for reactions 4 and 5 and other reactions of lesser importance, such as NO_2 + NO_3 = NO +
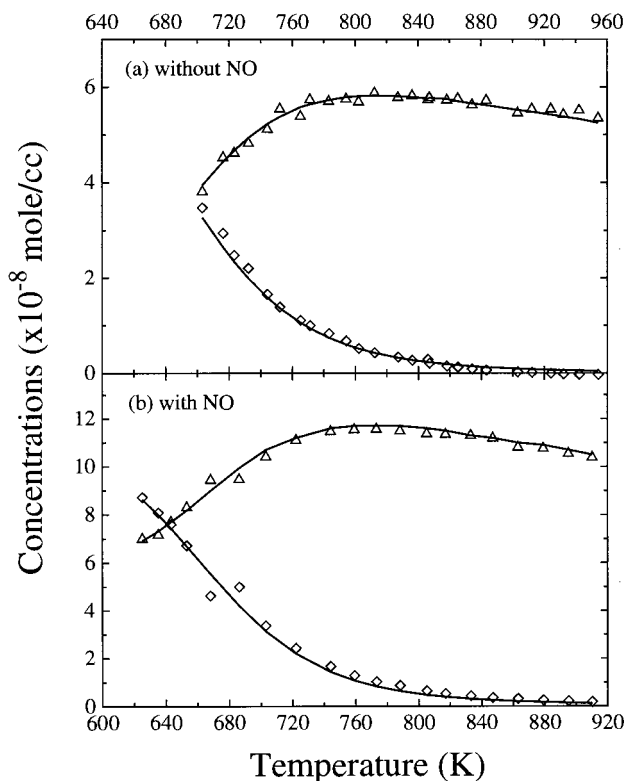
Thermal Reduction of NO$_2$ by H$_2$

J. Phys. Chem. A, Vol. 102, No. 49, 1998 **10101**

Figure 3. The concentration profiles of reactants and products measured in the pyrolysis of NO$_2$/Ar and NO$_2$/NO/Ar mixtures as functions of temperature: (△) NO; (◇) NO$_2$. (—) Modeled results using our k_4 value (see the Appendix). Experimental conditions are given in Table 1.
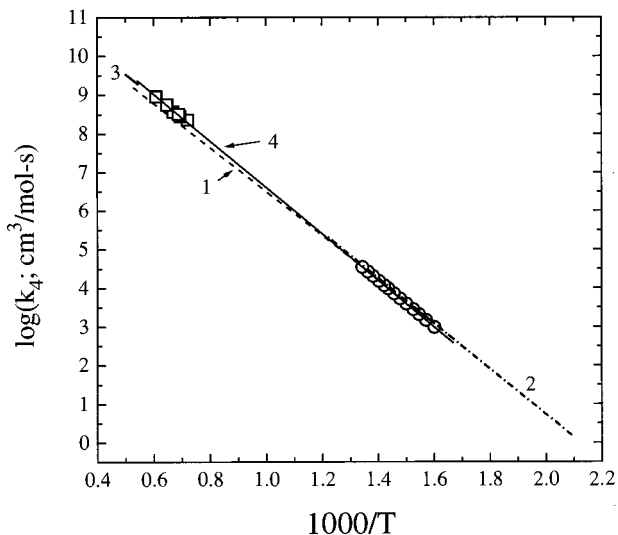

Figure 4. Arrhenius plot for the NO$_2$ + NO$_2$ → 2NO + O$_2$ reaction: (○) this work; (□), ref 27; 1, ref 23; 2, ref 28; 3, ref 29; 4, a combination of this work and ref 27.

TABLE 2: Comparison of the Rate Constant Expression for the NO$_2$ + NO$_2$ ⇌ 2NO + O$_2$ Reaction

	rate constant expression[a]	T (K)	P (Torr)	bath gas	ref
1	$1.63 \times 10^{12} \exp(-13\,150/T)$	300−2500			23
2	$3.08 \times 10^{12} \exp(-13\,540/T)$	473−823	10−252	N$_2$	28
3	$3.00 \times 10^{12} \exp(-13\,540/T)$	1830−2000		Ar	29
4	$2.00 \times 10^{12} \exp(-12\,580/T)$	1388−1640	228−2128	Ar	27
5	$4.16 \times 10^{12} \exp(-13\,840/T)$	625−954	760	Ar	this work
6	$4.51 \times 10^{12} \exp(-13\,890/T)$	625−1640	228−2128	Ar	this work[b]

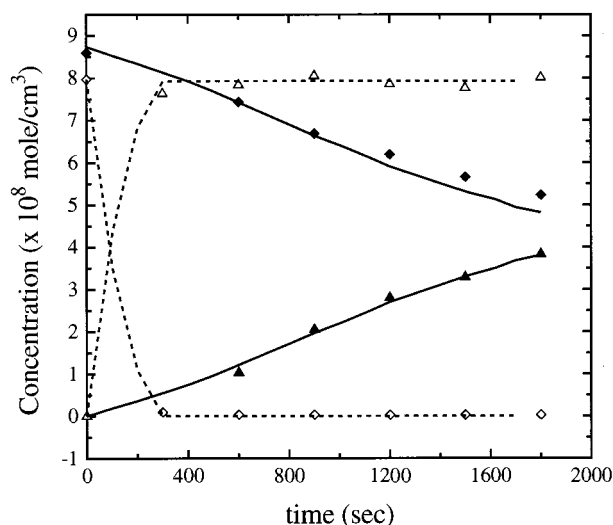[a] Rate constants are in the units of cm^3/(mol s). [b] Combination of items 4 and 5.

Figure 5. Concentration profiles of reactant (NO$_2$, ◇) and product (NO, △) as functions of residence time. Solid curves and filled symbols at 613 K; dashed curves and open symbols at 663 K. Curves are modeled results using our k_{-1} and k_7 values. Reaction conditions: NO$_2$ = 1.76 Torr, H$_2$ = 17.86 Torr, and Ar balanced to 760 Torr.

temperatures are shown in Figure 5, and the measured absolute concentrations of IR-active reactants and products from reactions without and with the added CO at a 1200 s residence time as a function of temperature are presented in Figures 6 and 7, respectively. As will be discussed later, these results, similar to those of the NO$_2$ determined by Ashmore and Levitt[22] by UV spectrophotometry presented in Figure 1, cannot be reasonably accounted for with the recommended rate constants for the key HONO reactions. In the following section, a possible cause of this discrepancy will be examined and discussed.

4. Discussion

As presented in the preceding section, the formation of NO and the decay of NO$_2$ in the pyrolysis of the NO$_2$/Ar and NO$_2$/NO/Ar mixtures can be well-described by the recommended rate constant[23] for the most influential channel:

$$NO_2 + NO_2 \rightleftarrows 2NO + O_2 \qquad (4)$$
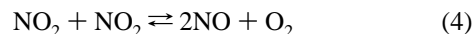
The purpose of NO addition in one of our reaction mixtures lies in minimizing the contribution of reaction 5. The result of our sensitivity analysis (not shown) clearly indicates that reaction 5 contributes negligibly to the formation of NO and the decay of NO$_2$ on account of the fast reverse reaction under our experimental conditions.

By adjusting k_4 to match the measured and predicted concentrations of NO and NO$_2$ at t = 900 and 1200 s over the temperature range 625−954 K, we obtained slightly revised

NO$_2$ + O$_2$ (6). To check the extent of deviation in k_4, we have utilized our NO and NO$_2$ concentrations to model the rate constant; the modeled results are summarized in Figure 4 and Table 2 for comparison with the existing kinetic data. The resulting rate constant from the combination of our data and the recently reported shock-tube data by Röhrig et al.[27] gave rise to k_4 = (4.51 ± 0.15) × 10^{12} exp[−(13 890 ± 27)/T] cm^3/(mol s); this rate constant was employed for further kinetic modeling.

The measured concentration−time profiles of NO and NO$_2$ from the pyrolysis of NO$_2$−H$_2$ mixtures at two specified

Figure 6. Concentration profiles of reactants and products as a function of the temperature measured in the pyrolysis of $H_2/NO_2/Ar$ mixtures: ($\triangle$) NO; ($\diamond$) NO_2. (—) Modeled results using our k_{-1} and k_7 values; (- - -) modeled results using the recommended rate constants for k_{-1} and k_7 (see the Appendix for these rate constants). Experimental conditions are given in Table 1.
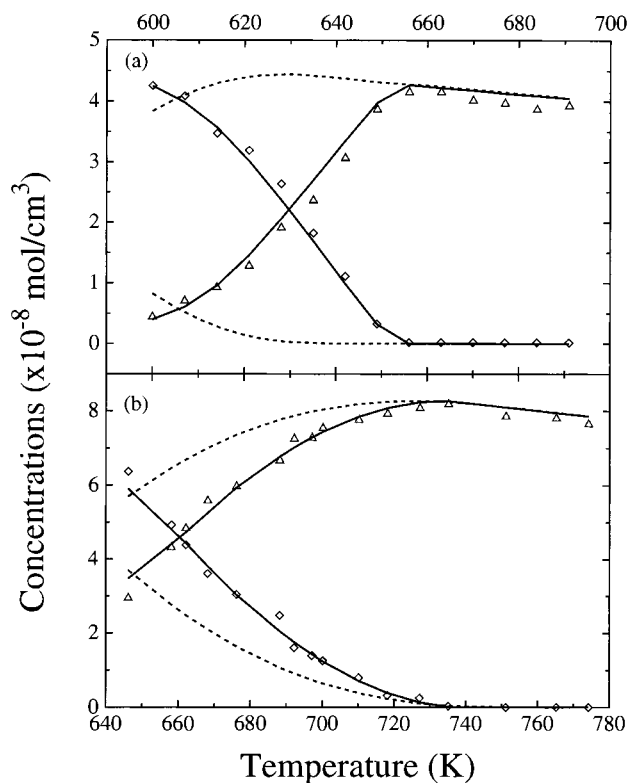

Figure 7. Concentration profiles of reactants and products as a function of the temperature measured in the pyrolysis of (a) $H_2/NO_2/CO/NO/Ar$ and (b) $H_2/NO_2/CO/Ar$ mixtures: ($\triangle$) NO; ($\diamond$) NO_2; ($\bigcirc$) CO; ($\square$) CO_2. (—) Modeled results using our k_{-1} and k_7 values; (- - -) modeled results using the recommended rate constants for k_{-1} and k_7 (see the Appendix). Experimental conditions are given in Table 1.

values for k_4 as given in Table 2 and Figure 4. Our low-temperature results compare reasonably with earlier data and can be correlated quite well with the recent high-temperature (1388−1640 K) shock-tube data of by Röhrig et al.[27] Combination of our results with ref 27 gave rise to the expression $k_4 = (4.51 \pm 0.15) \times 10^{12} \exp[-(13\,890 \pm 27)/T]$ cm^3/(mol s) covering the temperature range 625−1640 K.

The concentrations of NO_x and CO_x ($x = 1, 2$) measured in the pyrolysis of $NO_2/H_2/Ar$ mixtures without and with added CO are presented in Figures 6 and 7 for comparison with kinetically modeled values. The use of the recommended rate constants for key HONO reactions as given in the Appendix led to poor agreement with experimental results, particularly at lower temperatures. A much greater discrepancy was noted in our modeling of Ashmore and Levitt's result as mentioned in the Introduction (see Figure 1). The major process responsible for the deviation between experiment and modeling, according to the results of sensitivity analyses (see Figure 8), is the initiation reaction (−1).

The application of our theoretically predicted rate constant for reaction −1,[17] together with the predicted, much smaller rate constant for the self-reaction of HONO, reaction 7,[19] led to a considerably better agreement. In view of the improvement and the high sensitivity of the rates of NO_2 decay and those of NO and CO_2 formation to the initiation reaction, we attempted to adjust the values of k_{-1} to match the measured and modeled concentrations of NO_x and CO_x (in the CO-added experiments). The final values of k_{-1} are presented graphically in Figure 9. As is evident from the figure, the modeled results of k_{-1} (denoted by open circles) agree very closely with the theoretically predicted values (given by the dashed curve) for $NO_2 + H_2 \rightarrow HONO + H$ (reaction −1).

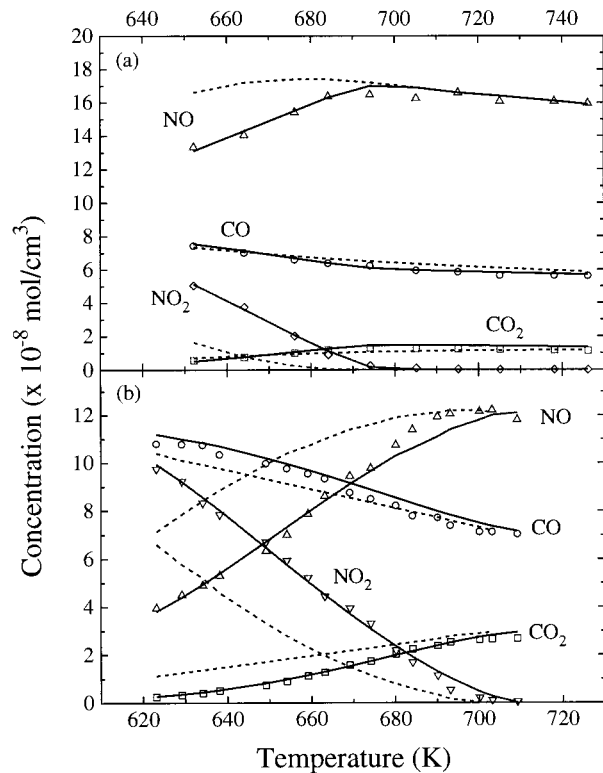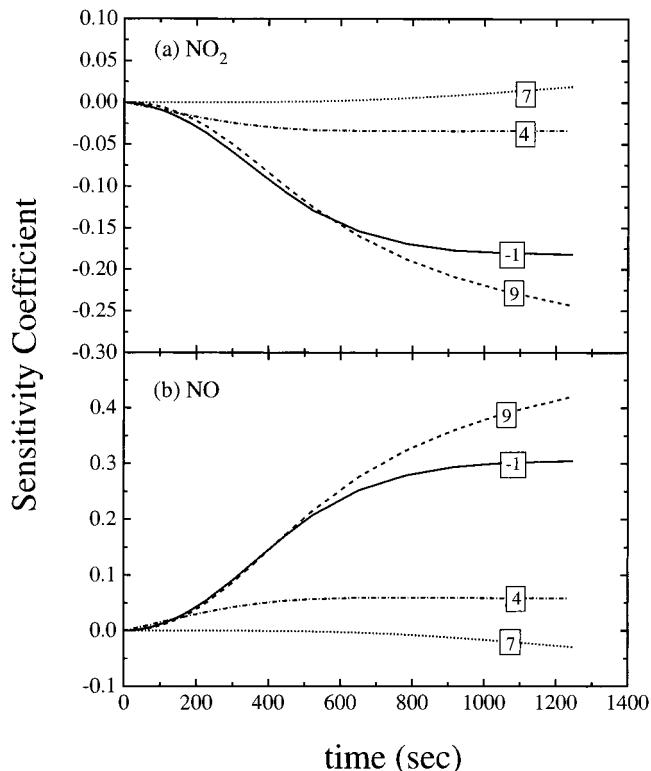**Figure 8.** Sensitivity analysis at $T = 630$ K for NO_2 and NO in the H_2/NO_2 system. Conditions are the same as Figure 6a given in Table 1.

The kinetically modeled results can be quantitatively accounted for by the theory with a slight upward adjustment of

APPENDIX. Reaction Mechanism and Rate Constants[a] Employed for Kinetic Modeling[b] of the H$_2$ + NO$_2$ System

	reactions	A	n	E_a	ref [c]
1	HONO + H $\rightleftharpoons$ H$_2$ + NO$_2$	1.46E+04	2.3	3433	d
−1	H$_2$ + NO$_2$ $\rightleftharpoons$ HONO + H	1.30E+04	2.8	29770	this work
		2.41E + 13	0.0	28810	23
2	HONO + H $\rightleftharpoons$ HNO + OH	5.64E+10	0.9	4969	17
3	HONO + H $\rightleftharpoons$ NO + H$_2$O	8.13E+06	1.9	3846	17
4	NO$_2$ + NO$_2$ $\rightleftharpoons$ NO + NO + O$_2$	4.51E+12	0.0	27600	this work
5	NO$_2$ + NO$_2$ $\rightleftharpoons$ NO$_3$ + NO	7.76E+11	0.0	23900	
6	NO$_3$ + NO$_2$ $\rightleftharpoons$ NO + NO$_2$ + O$_2$	4.90E+10	0.0	2940	
7	HONO + HONO $\rightleftharpoons$ NO + NO$_2$ + H$_2$O	9.69E+10	0.0	14132	19
		2.30E + 10	0.0	8400	23
8	HONO + NO$_2$ $\rightleftharpoons$ HNO$_3$ + NO	2.00E+11	0.0	32700	e
9	OH + H$_2$ $\rightleftharpoons$ H$_2$O + H	1.02E+08	1.6	3298	
10	H + NO$_2$ $\rightleftharpoons$ NO + OH	8.40E+13	0.0	0	
11	H + HNO$_3$ $\rightleftharpoons$ H$_2$ + NO$_3$	5.56E+08	1.5	16400	14
12	H + HNO$_3$ $\rightleftharpoons$ H$_2$O + NO$_2$	6.08E+01	3.3	6285	14
13	H + HNO$_3$ $\rightleftharpoons$ OH + HONO	3.82E+05	2.3	6976	14
14	H + O$_2$ + M $\rightleftharpoons$ HO$_2$ + M	2.10E+18	−1.0	0	
15	H + O$_2$ + N$_2$ $\rightleftharpoons$ HO$_2$ + N$_2$	6.70E+19	−1.4	0	
16	H + OH + M $\rightleftharpoons$ H$_2$O + M	1.60E+22	−2.0	0	
17	H$_2$ + O$_2$ $\rightleftharpoons$ OH + OH	1.70E+13	0.0	47780	
18	H$_2$O$_2$ + H $\rightleftharpoons$ H$_2$O + OH	1.00E+13	0.0	3576	
19	H$_2$O$_2$ + H $\rightleftharpoons$ HO$_2$ + H$_2$	1.70E+12	0.0	3755	
20	H$_2$O$_2$ + M $\rightleftharpoons$ OH + OH + M	1.30E+17	0.0	45500	
21	H$_2$O$_2$ + O $\rightleftharpoons$ HO$_2$ + OH	6.60E+11	0.0	3974	
22	H$_2$O$_2$ + OH $\rightleftharpoons$ H$_2$O + HO$_2$	7.80E+12	0.0	1330	
23	HNO + H $\rightleftharpoons$ NO + H$_2$	4.40E+11	0.7	650	
24	HNO + HNO $\rightleftharpoons$ N$_2$O + H$_2$O	4.00E+12	0.0	5000	
25	HNO + M $\rightleftharpoons$ H + NO + M	1.50E+16	0.0	48680	
26	HNO + NO $\rightleftharpoons$ N$_2$O + OH	2.00E+12	0.0	26000	
27	HNO + NO$_2$ $\rightleftharpoons$ HONO + NO	4.42E+04	2.6	4060	18
28	HNO + O $\rightleftharpoons$ NO + OH	1.00E+13	0.0	0	
29	HNO + O$_2$ $\rightleftharpoons$ NO + HO$_2$	1.00E+13	0.0	25000	
30	HNO + OH $\rightleftharpoons$ NO + H$_2$O	3.60E+13	0.0	0	
31	HO$_2$ + H $\rightleftharpoons$ H$_2$ + O$_2$	4.30E+13	0.0	1411	
32	HO$_2$ + H $\rightleftharpoons$ O + H$_2$O	3.00E+13	0.0	1721	
33	HO$_2$ + H $\rightleftharpoons$ OH + OH	1.70E+14	0.0	975	
34	HO$_2$ + HO$_2$ $\rightleftharpoons$ H$_2$O$_2$ + O$_2$	1.30E+11	0.0	−1630	
35	HO$_2$ + O $\rightleftharpoons$ OH + O$_2$	3.30E+13	0.0	0	
36	HO$_2$ + OH $\rightleftharpoons$ H$_2$O + O$_2$	2.90E+13	0.0	−497	
37	HONO + O $\rightleftharpoons$ NO$_2$ + OH	1.20E+13	0.0	6000	
38	HONO + OH $\rightleftharpoons$ NO$_2$ + H$_2$O	4.00E+12	0.0	0	
39	N + NO $\rightleftharpoons$ O + N$_2$	3.30E+12	0.3	0	
40	N + O$_2$ $\rightleftharpoons$ NO + O	6.40E+09	1.0	6280	
41	N + OH $\rightleftharpoons$ NO + H	3.80E+13	0.0	0	
42	N$_2$O + H $\rightleftharpoons$ N$_2$ + OH	3.30E+10	0.0	4729	
43	N$_2$O + O $\rightleftharpoons$ N$_2$ + O$_2$	1.40E+12	0.0	10800	
44	N$_2$O + O $\rightleftharpoons$ NO + NO	2.90E+13	0.0	23150	
45	NO + OH + M $\rightleftharpoons$ HONO + M	5.08E+23	−2.5	−68	
46	NO$_2$ + M $\rightleftharpoons$ NO + O + M	8.10E+14	0.0	52500	
47	NO$_2$ + O + M $\rightleftharpoons$ NO$_2$ + M	1.00E+28	−4.1	2470	
48	NO$_2$ + O $\rightleftharpoons$ NO + O$_2$	3.90E+12	0.0	−238	
49	NO$_3$ + H $\rightleftharpoons$ NO$_2$ + OH	6.00E+13	0.0	0	
50	NO$_3$ + HO$_2$ $\rightleftharpoons$ NO$_2$ + O$_2$ + OH	1.50E+12	0.0	0	
51	NO$_3$ + O $\rightleftharpoons$ NO$_2$ + O$_2$	1.00E+13	0.0	0	
52	NO$_3$ + OH $\rightleftharpoons$ NO$_2$ + HO$_2$	1.00E+13	0.0	0	
53	O + H$_2$ $\rightleftharpoons$ H + OH	5.00E+04	2.7	6300	
54	O + O + M $\rightleftharpoons$ O$_2$ + M	1.90E+13	0.0	−1788	
55	O + OH $\rightleftharpoons$ H + O$_2$	2.00E+14	−0.4	0	
56	OH + HNO$_3$ $\rightleftharpoons$ H$_2$O + NO$_3$	1.03E+10	0.0	−1240	
57	OH + NO$_2$ + M $\rightleftharpoons$ HNO$_3$ + M	6.69E+30	0.0	1160	21
58	OH + NO$_2$ $\rightleftharpoons$ HO$_2$ + NO	1.45E+13	0.0	−477	21
59	OH + OH $\rightleftharpoons$ H$_2$O + O	4.30E+03	2.7	−2486	
60	OH + CO $\rightleftharpoons$ CO$_2$ + H	2.47E+06	1.6	−845	
61	HCO + M $\rightleftharpoons$ H + CO + M	1.90E+17	−1.0	17200	
62	H + CH$_2$O $\rightleftharpoons$ H$_2$ + HCO	2.28E+10	1.1	3279	
63	H + HCO $\rightleftharpoons$ H$_2$ + CO	9.00E+13	0.0	0	
64	HCO + HCO $\rightleftharpoons$ CH$_2$O + CO	3.00E+13	0.0	0	
65	HCO + HNO $\rightleftharpoons$ CH$_2$O + NO	2.00E+11	0.7	0	
66	HCO + NO $\rightleftharpoons$ HNO + CO	7.20E+13	−0.4	0	
67	OH + HCO $\rightleftharpoons$ H$_2$O + CO	5.00E+13	0.0	0	

[a] Rate constants defined by $k = AT^n \exp(-E_a/RT)$ are given in units of cm^3, mol, and s; E_a is in units of cal/mol. [b] With the CHEMKIN program (ref 32). [c] Reference 6, except those noted. [d] The rate constant was reevaluated by increasing $E_1^\circ = 7.2$ to 7.7 kcal/mol with tunneling corrections. [e] Unpublished work.
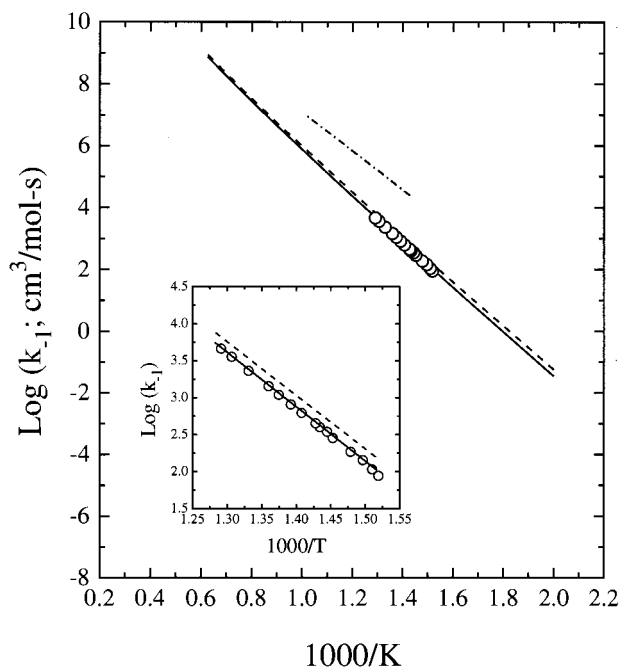
Figure 9. Arrhenius plot for the $H_2 + NO_2 \rightarrow H + HONO$ reaction: (○) this work; solid and dashed curves, theoretically predicted values (see the text for explanation); dash−dotted curve, ref 23.

the predicted 0 K energy barrier from $E^{\circ}_{-1} = 32.5$ to 33.0 kcal/mol. The resulting expression given by the solid curve, which matches the modeled data quatitatively, can be represented by $k_{-1} = (1.30 \times 10^4)T^{2.76} \exp(-14\,980/T)$ cm^3/(mol s).

In the same figure the recommended rate constant for k_{-1} (given by the dash−dotted line) is also plotted for comparison. Our new rate constant is lower than the recommended value by a factor of 75 at 650 K. The employment of our smaller rate constant for the initiation process as well as the smaller, predicted HONO + HONO rate constant, allows us to satisfactorily account for not only our own $H_2 + NO_2$ and $H_2 + NO_2 + CO$ data but also those of Ashmore and Levitt[22] for the $H_2 + NO_2$ reaction using considerably higher reactant concentrations, as illustrated in Figure 1.

In Figure 10, we also compare the predicted initial rates of the $H_2 + O_2$ reaction at 662 K for mixtures containing 200 Torr of H_2 and 100 Torr of O_2, with varying amounts of NO_2, originaly reported by Crist and Wertz in 1939.[30] Significantly, the experimentally observed V-shaped NO_2 dependency resulting from the combination of a deceleration at low NO_2 concentration (≤5 Torr) and an acceleration at high NO_2 concentration can be reasonably explained by our mechanism. The deceleration of the initial rate is likely caused by the chain-termination step

$$OH + NO_2 + M \rightarrow HNO_3 + M$$

whereas the acceleration effect at higher NO_2 concentrations probably results from the contribution of reactions −1 and 10, which generate more H and OH by

$$NO_2 + H_2 \rightarrow HONO + H \quad\quad (-1)$$

$$H + NO_2 \rightarrow OH + NO \quad\quad (10)$$
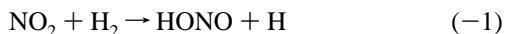
5. Concluding Remarks

The results of this study on the thermal reaction of NO_2 with and without added NO and the reduction of NO_2 by H_2 with and without added CO employing the technique of pyrolysis/
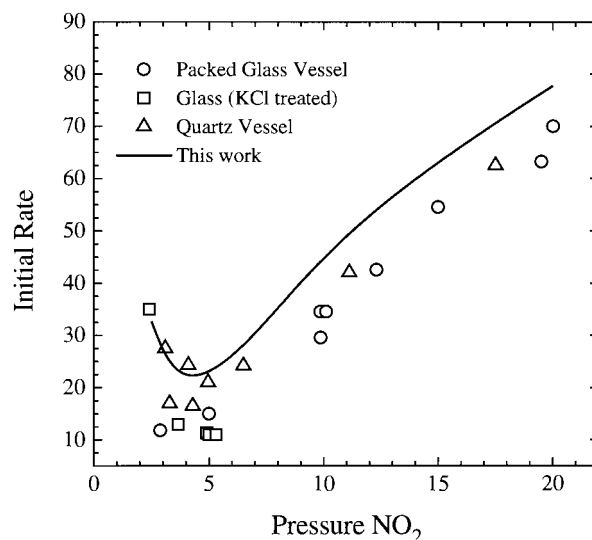

Figure 10. Initial rates of the $H_2 + NO_2$ reaction as a fuction of NO_2. Reaction mixtures: H_2 = 200 Torr, O_2 = 100 Torr, reaction time = 30 min. Initial rate is the pressure change of H_2 for 30 min. (—) Modeling result using our k_{-1} and k_7 values given in the Appendix. The experimental data were reproduced from ref 30.

FTIR spectrometry indicate that the rate constant for the bimolecular self-reaction of NO_2 given in the literature is very reliable. The measured NO and NO_2 concentrations could be quantitatively accounted for with the recommended value.[23] The kinetics for the reaction of NO_2 with H_2, on the other hand, could not be satisfactorily described by the existing rate constants for the key HONO reactions, particularly H + HONO $\rightleftarrows H_2 + NO_2$ (reaction −1), whose reverse process initiates the reduction reaction of NO_2. The application of our theoretically predicted k_1 (or k_{-1}), in conjunction with the smaller theoretical rate constant for the self-reaction of HONO, led to near quantitative agreement between the modeled and measured NO_x and CO_x (in the CO added case) concentrations; $x = 1, 2$. By matching the predicted and observed data, we obtained the following expression for k_{-1}

$$k_{-1} = (1.30 \times 10^4)T^{2.76} \exp(-14\,980/T) \text{ cm}^3/\text{(mol s)}$$

for 500 K < T < 2000 K. The above equation was computed theoretically by ab inito MO/TST calculations using our previously obtained transition-state parameters[17] with a small adjustment for the predicted reaction barrier from 32.5 to 33.0 kcal/mol for reaction −1.

Theoretically, reaction −1 produces *cis*-HONO, which is less stable than *trans*-HONO by 0.6 kcal/mol (cf. the JANAF value of 0.5 kcal/mol[31]). The production of *trans*-HONO requires a much higher activation energy (10 kcal/mol), however.[17] It is thus unimportant to the low-temperature NO_2 reduction process. In view of the presence of these two isomers in the present system, we have created separate thermochemistry files for them and differentiate them in our kinetic modeling by including the very fast isomerization process

$$\textit{trans}\text{-HONO} + M \rightleftarrows \textit{cis}\text{-HONO} + M$$
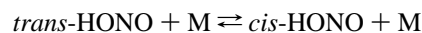
using the theoretically predicted (G2/RRKM) rate constant, k_{iso} = $(1.06 \times 10^{20})T^{-1.72} \exp(-6730/T)$ cm^3/(mol s), and the different rate constants for the cross-reaction and self-reactions of the HONO isomers.[19] Our modeling using the refined mechanism gave essentially the same results as those reported above. Accordingly, for kinetic modeling above room temper-

ature, there is no need to differentiate these isomers because of the small energy difference and the small energy barrier for the isomerization process ($E_0 = 9.1$ kcal/mol).

It should also be mentioned that the addition of CO to the NO$_2$−H$_2$ system (which provides additional kinetic data for mechanistic validation) does not alter the rates of NO formation and NO$_2$ decay significantly (as revealed by the result of kinetic modeling with and without CO) under our experimental conditions. This is understandable because of the rapid regeneration of OH by H + NO$_2$ → OH + NO, after it is converted to H by OH + CO. If the OH regeneration process is slow, then the effect of CO will be noticeable kinetically.

References and Notes

(1) Diau, E. M. G.; Lin, M. C.; He Y.; Melius, C. F. *Prog. Energy Combust. Sci*. **1995**, *21*, 1.

(2) Diau, E. W. G.; Halbgewachs, M. J.; Smith A. R.; Lin, M. C. *Int. J. Chem. Kinet*. **1995**, *27*, 867.

(3) Halbgewachs, M. J.; Diau, E. W. G.; Mebel, A. M.; Lin, M. C.; Melius, C. F. *26th Symposium (Intl) on Combustion*; The Combustion Institute: Pittsburgh, PA, 1996; p 2109.

(4) Park, J.; Lin, M. C. *Int. J. Chem. Kinet*. **1996**, *28*, 879.

(5) Park, J.; Lin, M. C. *J. Phys. Chem*. **1996**, *100*, 3317.

(6) Park, J.; Lin, M. C. *J. Phys. Chem*. **1997**, *A101*, 5.

(7) Park, J.; Lin, M. C. *J. Phys. Chem*. **1997**, *A101*, 2643.

(8) Park, J.; Lin, M. C. Combustion Technogies for a Clean Environment. In *Energy, Combustion and the Environment*; 1998; Vol. 4, in press.

(9) Lin, M. C.; He, Y.; Melius, C. F. *Int. J. Chem. Kinet*. **1992**, *24*, 489.

(10) Mebel, A. M.; Morokuma, K.; Lin, M. C. *J. Chem. Phys*. **1994**, *101,* 3916.

(11) Mebel, A. M.; Morokuma, K.; Lin, M. C.; Melius, C. F. *J. Phys. Chem*. **1990**, *99*, 1900.

(12) Mebel, A. M.; Diau, E. W. G.; Lin, M. C.; Morokuma, K. *J. Phys. Chem*. **1996**, *100*, 7517.

(13) Mebel, A. M.; Hsu, C.-C.; Lin, M. C.; Morokuma, K. *J. Chem. Phys*. **1995**, *103*, 5640.

(14) Boughton, J. W.; Kristyan, S.; Lin, M. C. *Chem. Phys*. **1997**, *214*, 219.

(15) Mebel, A. M.; Lin, M. C.; Morokuma, K.; Melius, C. F. *Int. J. Chem. Kinet*. **1996**, *28*, 693.

(16) Thaxton, A. G.; Hsu, C.-C.; Lin, M. C. *Int. J. Chem. Kinet*. **1997**, *29*, 245.

(17) Hsu, C.-C.; Lin, M. C.; Mebel, A. M.; Melius, C. F. *J. Phys. Chem*. **1997**, *A101*, 60.

(18) Mebel, A. M.; Lin, M. C.; Morokuma, K. *Int. J. Chem. Kinet*., in press.

(19) Mebel, A. M.; Lin, M. C.; Melius, C. F. *J. Phys. Chem*. **1998**, *A102*, 1803.

(20) Hsu, C.-C.; Boughton, J. W.; Mebel, A. M.; Lin, M. C. In *Challenges in Propellant and Combustion: 100 Years after Nobel*; Begell House, Inc.: New York, Aug. 1997; pp 48−57.

(21) Chakraborty, D.; Park, J.; Lin, M. C. *Chem. Phys*. **1998**, *231*, 39.

(22) Ashmore, P. G.; Levitt, B. P. *Trans. Faraday Soc*. **1956**, *52*, 835.

(23) Tsang, W.; Herron, J. T. *J. Phys. Chem. Ref. Data* **1991**, *20*, 609.

(24) Aldridge, H. K.; Liu, X.; Lin, M. C.; Melius, C. F. *Int. J. Chem. Kinet*. **1991**, *23*, 947.

(25) He, Y.; Liu, X.; Lin, M. C.; Melius, C. F. *Int. J. Chem. Kinet*. **1993**, *25*, 845.

(26) Park, J.; Dyakov, I. V.; Mebel, A. M.; Lin, M. C. *J. Phys. Chem*., **1997**, *A101*, 6043.

(27) Röhrig, M.; Peterson, E. L.; Davision D. F.; Hanson, R. K. *Int. J. Chem. Kinet*. **1997**, *29*, 483.

(28) Ashmore, P. G.; Levitt, B. T. *Trans. Faraday Soc*. **1962**, *58*, 253.

(29) Zimet, E. *J. Chem. Phys*. **1970**, *53*, 515.

(30) Crist, R. H.; Wertz, J. E. *J. Chem. Phys*. **1939**, *7,* 719.

(31) Chase, M. W. JANAF Thermochemical Tables, 3rd ed. *J. Phys. Chem. Ref. Data* **1985**, *14*, Suppl 1.

(32) Luts, A. E.; Lee, R. K.; Miller, J. A. *SENKIN: A FORTRAN Program for Predicting Homogeneous Gas-Phase Chemical Kinetics with Sensitivity Analysis*; Sandia National Laboratories Report No. SANDDIA 89-8009, 1989.